

# Argon-based atmospheric pressure plasma enhances early bone response to rough titanium surfaces

Paulo G. Coelho,<sup>1</sup> Gabriela Giro,<sup>2</sup> Hellen S. Teixeira,<sup>1</sup> Charles Marin,<sup>3</sup> Lukas Witek,<sup>1</sup> Van P. Thompson,<sup>1</sup> Nick Tovar,<sup>1</sup> Nelson R. F. A. Silva<sup>4</sup>

<sup>1</sup>Department of Biomaterials and Biomimetics, New York University, New York, New York

<sup>2</sup>Department of Oral Diagnosis and Surgery, Araraquara Dental School, UNESP, Universidade Estadual Paulista, Araraquara, SP, Brazil

<sup>3</sup>Department of Dentistry, Universidade Federal de Santa Catarina, Florianópolis, SC, Brazil

<sup>4</sup>Department of Prosthodontics, New York University, New York, New York

Received 30 September 2011; revised 21 January 2012; accepted 7 February 2012

Published online 10 April 2012 in Wiley Online Library (wileyonlinelibrary.com). DOI: 10.1002/jbm.a.34127

**Abstract:** This study investigated the effect of an Argon-based atmospheric pressure plasma (APP) surface treatment operated chairside at atmospheric pressure conditions applied immediately prior to dental implant placement in a canine model. Surfaces investigated comprised: rough titanium surface (Ti) and rough titanium surface + Argon-based APP (Ti-Plasma). Surface energy was characterized by the Owens-Wendt-Rabel-Kaelble method and chemistry by X-ray photoelectron spectroscopy (XPS). Six adult beagles dogs received two plateau-root form implants ( $n = 1$  each surface) in each radii, providing implants that remained 1 and 3 weeks *in vivo*. Histometric parameters assessed were bone-to-implant contact (BIC) and bone area fraction occupancy (BAFO). Statistical analysis was performed by Kruskal-Wallis (95% level of significance) and Dunn's post-hoc test. The XPS analysis showed peaks of Ti, C, and O for the Ti and Ti- Plasma surfa-

ces. Both surfaces presented carbon primarily as hydrocarbon (C—C, C—H) with lower levels of oxidized carbon forms. The Ti-Plasma presented large increase in the Ti (+11%) and O (+16%) elements for the Ti- Plasma group along with a decrease of 23% in surface-adsorbed C content. At 1 week no difference was found in histometric parameters between groups. At 3 weeks significantly higher BIC (>300%) and mean BAFO (>30%) were observed for Ti-Plasma treated surfaces. From a morphologic standpoint, improved interaction between connective tissue was observed at 1 week, likely leading to more uniform and higher bone formation at 3 weeks for the Ti-Plasma treated implants was observed. © 2012 Wiley Periodicals, Inc. *J Biomed Mater Res Part A*: 100A: 1901–1906, 2012.

**Key Words:** endosseous implant, surface treatment, atmospheric pressure plasma, osseointegration

**How to cite this article:** Coelho PG, Giro G, Teixeira HS, Marin C, Witek L, Thompson VP, Tovar N, Silva NRFA. 2012. Argon-based atmospheric pressure plasma enhances early bone response to rough titanium surfaces. *J Biomed Mater Res Part A* 2012;100A:1901–1906.

## INTRODUCTION

Biomaterials surfaces are the first part of an implantable device to interact with the host and have therefore been extensively investigated in an attempt to induce a favorable early host-to-implant response.<sup>1</sup> The rationale for surface modification focuses upon implant interaction with biofluids, in hopes of positively altering the cascade of events that leads to bone healing and initiates interaction with the device.<sup>2</sup>

The literature<sup>3,4</sup> covers a large number of possibilities included in surface modifications, with a general consensus that certain alterations in surface texture (roughening) and surface chemistry (adding various forms of calcium phosphate [CaP]-based bioactive ceramics) favor the desired

early host-to-implant response.<sup>3,5,6</sup> Historically, implantable device surfaces evolved from smooth to textured/rough, and recent research points toward chemistry modification of moderately rough surfaces.<sup>3–7</sup> However, while improvements in host-to-implant response have been experimentally demonstrated with implant surface texture or chemistry modifications,<sup>8–10</sup> there is no consensus concerning which surface roughness and/or chemistry combination will result in the fastest and highest-quantity/quality osseointegration. In most cases, combinations of texture and chemistry known to hasten the host response are proprietary product-specific processes controlled by manufacturers during fabrication and are not general-purpose processes widely available to the surgical community.

**Correspondence to:** Paulo G. Coelho, New York University College of Dentistry, 345E 24th Street, Room 813a, New York, NY 10010, USA; e-mail: pgcoelho@nyu.edu

Contract grant sponsors: INP Greifswald (KD Weltman); Bicon LLC (Boston, MA); Department of Biomaterials and Biomimetics; New York University

The approach to create surface treatments that have the potential to be applied to any dental implant have been attempted since the early days of dental implantology research. The early equipment used large thermal or radio frequency plasma devices that either operated at high temperatures or under low pressures. They suffered from operational inconsistency and its economic viability kept these early-stage implant surface treatments from being accepted into the mainstream market.

The plasma state is often referred to as the 4th state of matter. A plasma is characterized by the presence of positive and/or negative ions and charged electrons in a neutral background gas.<sup>11</sup> Plasmas can be categorized as either “thermal (or hot) plasmas” (such as those historically utilized for plasma spraying hydroxyapatite coatings on implant surfaces) or “atmospheric pressure (or cold) plasmas” (APPs). The main constituents of plasmas are ions, electrons, and neutrals in thermodynamic equilibrium. In APPs, most of the energy is put into the electron component which can drive “high-temperature” chemistry allowing surface activation/modification while operating at low ambient temperatures.<sup>12</sup> Recently, the microplasma APPs utilized in the present work have successfully reached clinical technological significance, as it has been built in small dimensions allowing its portability in the clinical setting and have been proven to provide enough energy for increasing surface energy while presenting safe operation at atmospheric conditions (unlike previous radiofrequency technology that required low pressures).<sup>13</sup>

Atmospheric pressure plasmas used in biomedical applications have shown to effectively change the energy and chemistry of surfaces due to the high concentration of reactive species that are generated.<sup>14,15</sup> Recent work has shown that mixtures of rare gases such as argon (Ar) and oxygen are suitable as metastable rare gas species (carriers of a significant amount of energy), leading to the formation of reactive oxygen species via energy transfer reactions.<sup>14,15</sup> Thus, depending on plasma set up and chemistry, the incorporation of reactive species and further surface cleaning may result in increased levels of surface reactivity and energy that can be applied immediately prior to implant placement. This efficient and cost-effective process presents a potential benefits to any commercially available implant surface.

The objective of this investigation was to histometrically evaluate the effect of an onsite Ar-based APP treatment onto an alumina-blasted/acid-etched dental implant surface performed immediately prior to implantation and compare it to a nontreated control, in a beagle dog model.

## MATERIALS AND METHODS

This study utilized plateau root form endosseous Ti-6Al-4V implants of 3.5 mm in diameter by 8 mm in length (the implant plateaus resulted in healing chambers that are approximately 200  $\mu\text{m}$  depth by 400  $\mu\text{m}$  in height, total 8 chambers per implant). The investigated implant surface treatment groups comprised: alumina-blasted/acid-etched (AB/AE) (Integra-Ti<sup>TM</sup>, Bicon LLC, Boston) and the same AB/AE in addition to atmospheric pressure plasma (APP)

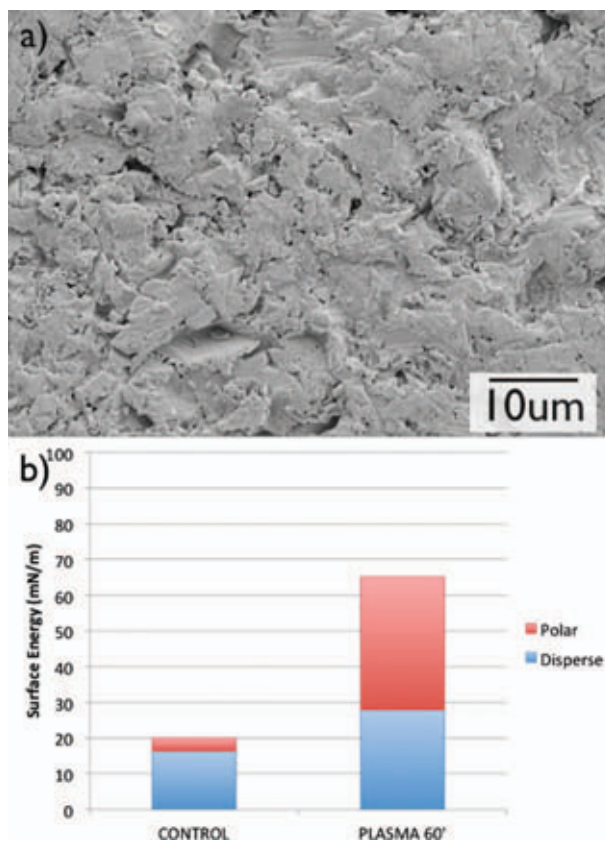


**FIGURE 1.** (a) Scanning electron microscopy micrograph of the Ar-based APP treated implant surface and (b) surface energy measurements of both surfaces used in this study. [Color figure can be viewed in the online issue, which is available at [wileyonlinelibrary.com](http://wileyonlinelibrary.com).]

(CaP-Plasma) treatment with Ar gas for a period of 60 s per quadrant with a KinPen<sup>TM</sup> device (INP-Greifswald, Germany). The latter implant surfaces were plasma treated immediately prior to implantation, and no attempt was made to prevent chemical species adsorption in the surgical setting. A scanning electron micrograph of the Ar-based APP-treated implant surface is presented in Figure 1(a). Previous surface characterization work by atomic force microscopy has shown that the mean average surface roughness ( $\pm$  standard deviation) was approximately  $0.66 \pm 0.10 \mu\text{m}$ .<sup>8</sup>

In order to assess the surface energy (SE) of both surfaces, the Owens-Wendt-Rabel-Kaelble (OWRK) method was utilized.<sup>16</sup> Totally, 500  $\mu\text{L}$  droplets of distilled water, ethylene glycol, and diiodomethane were deposited on the surface of each implant group with a micro-pipette (OCA 30, Data Physics Instruments GmbH, Filderstadt, Germany). Images were captured and analyzed using software (SCA30, version 3.4.6 build 79). The relationship between the contact angle and SE was determined, and the SE was calculated by  $\gamma_L = \gamma_L^D + \gamma_L^P$ , where  $\gamma_L$  is the SE,  $\gamma_L^D$  is the disperse component, and  $\gamma_L^P$  is the polar component.

Surface specific chemical assessment was performed by X-ray photoelectron spectroscopy (XPS). The implants ( $n = 3$ , each group) were inserted in a vacuum transfer chamber and degassed to  $10^{-7}$  torr. The samples were then transferred

under vacuum to a Kratos Axis 165 multitechnique XPS spectrometer (Kratos Analytical, Chestnut Ridge, NY). Survey and high-resolution spectra were obtained using a 165 mm mean radius concentric hemispherical analyzer operated at constant pass energy of 160 eV for survey and 80 eV for high resolution scans. The take off angle was 90° and a spot size of 150 μm × 150 μm was used. The implant surfaces were evaluated at various locations.

The *in vivo* study comprised of six adult male beagles dogs with ~1.5 years of age. The experimental protocol received the approval of the École Nationale Vétérinaire d'Alfort (Maisons-Alfort, Val-de-Marne, France).

All surgical procedures were performed under general anesthesia. The preanesthetic procedure comprised of an intramuscular (IM) administration of atropine sulfate (0.044 mg/kg) and xylazine chlorate (8 mg/kg). General anesthesia was then obtained following an IM injection of ketamine chlorate (15 mg/kg). Following hair shaving, skin exposure, and antiseptic cleaning with iodine solution at the surgical and surrounding area, a 5-cm incision at the skin level was performed. Then, a flap was reflected and the radius diaphysis exposed.

Two implants were placed along each limb at the center of the radius diaphysis. The different implant surfaces (Ti or Ti-Plasma) were alternately placed from proximal to distal at distances of 1 cm from each other along the central region of the bone. The start surface site was alternated between animals. The implant distribution resulted in an equal number of treated and nontreated implants per time point. Animals were euthanized at 1 and 3 week time points.

The initial drilling was performed by a 2 mm diameter pilot drill at 1200 rpm under saline irrigation. Then, slow speed sequential drilling with burs of 2.5, 3.0, and 3.5 mm was performed at 800 rpm under saline irrigation. The implants were then press fit into the osteotomy sites by manual pressure. Standard layered suture techniques were utilized for wound closure (4-0 vicryl- internal layers, 4-0 nylon-the skin). Post-surgical medication included antibiotics (penicillin, 20,000 UI/Kg) and analgesics (ketoprofen, 1 mL/5 kg) for a period of 48 h postoperatively. Euthanasia was performed by anesthesia overdose at 1 and 3 weeks after the first surgical procedure.

At necropsy, the limbs were retrieved by sharp dissection; the soft tissue was removed by surgical blades. The bone blocks were kept in 10% buffered formalin solution for 24 h, washed in running water for 24 h, and gradually dehydrated in a series of alcohol solutions ranging from 70 to 100% ethanol. Following dehydration, the samples were embedded in a methacrylate-based resin (Electron Microscopy Science, Hatfield, PA) according to the manufacturer's instructions. The blocks were then cut into slices (~300 μm thickness) aiming the center of the implant along its long axis with a precision diamond saw (Isomet 2000, Buehler, Lake Bluff, USA), glued to acrylic plates with an acrylate-based cement (Technovit 7210 VLC, Heraeus Kulzer GmbH, Wehrheim, Germany), and a 24-h setting time was allowed prior to grinding and polishing. The sections were then reduced to a final thickness of ~30 μm by means of a

series of SiC abrasive papers (280, 400, 800, 1200, 1500, and 2500 grit) (Buehler, Lake Bluff, IL) in a grinding/polishing machine (Metaserv 3000, Buehler, Lake Bluff, USA) under water irrigation. The sections were then toluidine blue stained and referred to optical microscopy evaluation. The histologic features were evaluated at 50–200× magnification (Leica DM2500M, Leica Microsystems GmbH, Wetzlar, Germany).

The bone-to-implant contact (BIC) was determined at 50-200X magnification (Leica DM2500M, Leica Microsystems GmbH, Wetzlar, Germany) by means of computer software (Leica Application Suite, Leica Microsystems GmbH, Wetzlar, Germany). The regions of bone-to-implant contact along the implant perimeter were subtracted from the total implant perimeter, and calculations were performed to determine the BIC percentage. The bone area fraction occupancy (BAFO) between plateaus was determined at 100× magnification with the same microscope and software. The percentage areas occupied by bone were calculated from the total area within the healing chambers.<sup>17</sup>

Statistical analysis was performed by Kruskal-Wallis at 95% level of significance and Dunn's post-hoc test. The analysis employed IBM SPSS Statistics, v. 19 (IBM, New York, NY).

## RESULTS

The surface energy assessments showed an increase in both polar and disperse components for the Ti-Plasma group [Fig. 1(b)] compared with the Ti group. The XPS survey analysis of the implant surface showed peaks of Ti and O for the Ti and Ti- Plasma surfaces. High-resolution spectrum evaluation showed that for both surfaces carbon was observed primarily as hydrocarbon (C–C, C–H) with lower levels of oxidized carbon forms. XPS detected a large increase in the Ti (+11%) and O (+16%) elements for the Ti-Plasma group along with a decrease of 23% in surface-adsorbed C content.

The surgical procedures and follow-up demonstrated no complications or other clinical concerns, and no implant was excluded due to clinical instability (determined after euthanization).

At 1 week the histologic sections of the Ti-Plasma group showed initial signs of bone formation adjacent to the implant surface and the presence of layers of early connective tissue (stroma) filling the region between plateaus (Fig. 2). In contrast, the Ti group presented the stroma collapsed to the center of the plateau (Fig. 2). At 3 weeks, bone formation was observed throughout the healing chambers of both groups (Fig. 2).

No significant difference was found for BIC and BAFO between surfaces at 1 week [Fig. 3(a,b), respectively]. At 3-weeks *in vivo*, bone formation in close contact to the implant surface (BIC) was strongly evidenced to the Ti-Plasma group [Fig. 3(a)], where an increase of over 300% was observed relative to the control ( $p < 0.001$ ). No significant differences were observed in BAFO ( $p > 0.14$ ) although an improvement of 30% was observed for the Ti-Plasma group [Fig. 3(b)].

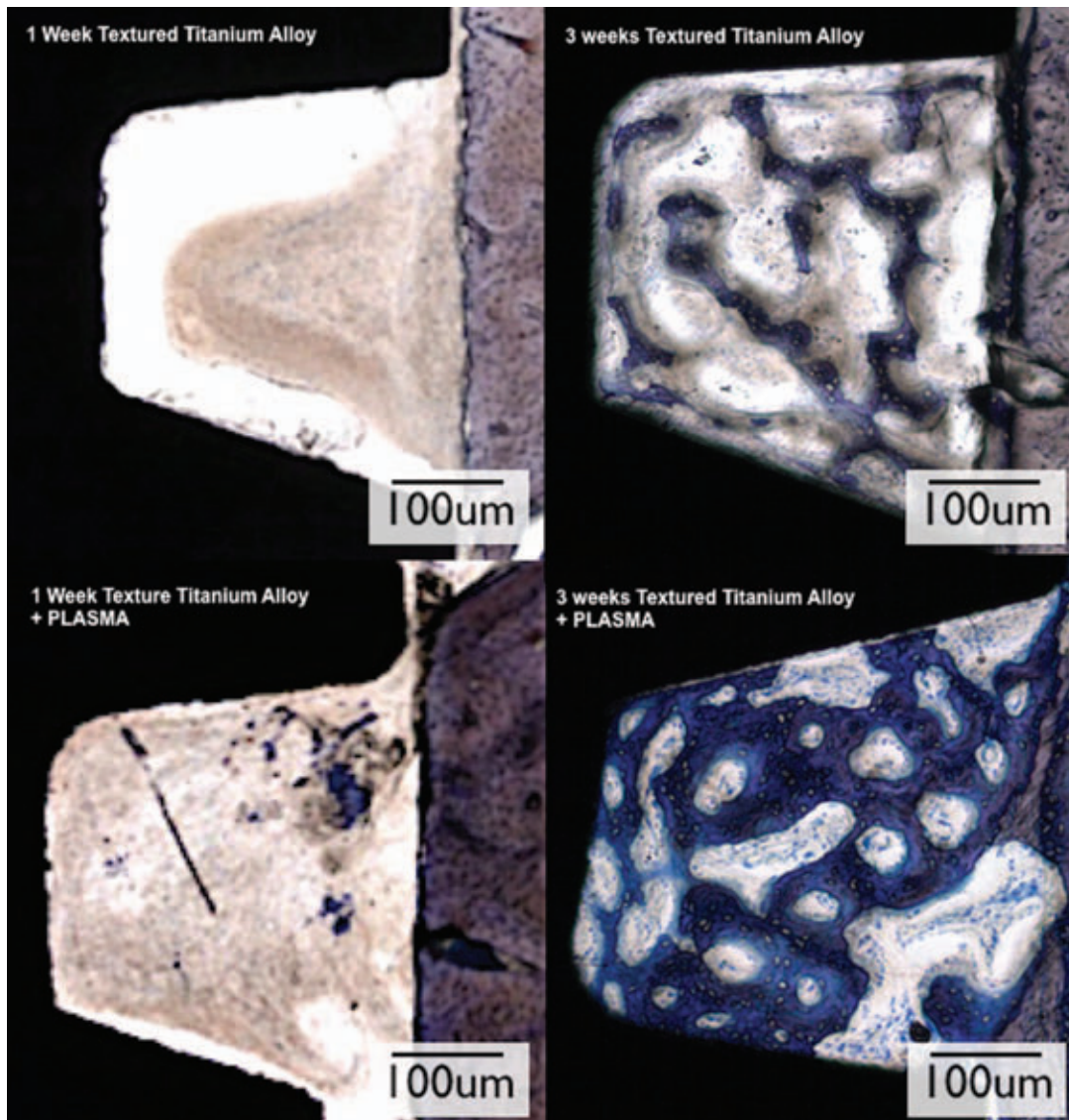


**FIGURE 2.** Representative overview of the histological micrographs of the plateaus at 1 and 3 weeks experimental periods at  $\times 200$  magnification. At 1 week, the histologic sections of the Ti-Plasma group showed initial signs of bone formation adjacent to the implant surface and the presence of layers of early connective tissue (stroma) filling the region between plateaus. In contrast, the Ti group presented the stroma collapsed to the center of the plateau. At 3 weeks, bone formation was observed throughout the healing chambers of both groups. [Color figure can be viewed in the online issue, which is available at [wileyonlinelibrary.com](http://wileyonlinelibrary.com).]

## DISCUSSION

To date, implant surfaces have been both cleaned and/or sterilized by radiofrequency plasma devices or plasma coated with bioactive ceramics with high temperature plasma sources.<sup>8</sup> Unlike previous plasma technology, where specialized equipment environment was required to allow low pressure levels and high temperature conditions, APPs can drive “high-temperature” chemistry at ambient temperatures at atmospheric pressure.<sup>12</sup> Thus, depending on plasma set up and chemistry, a wide range of implant surface alterations are achievable and may be utilized at the operating room immediately prior to implant placement under atmospheric conditions (these units may be fabricated in portable sizes). This study characterized surface energy and chemis-

try in AB/AE surfaces and its effect on the early bone to implant response in a beagle dog model.

The SEM and previous<sup>8</sup> atomic force microscopy assessment showed that the roughness of this implant surfaces were similar to that of several other commercially available products.<sup>3</sup> The surface energy assessment prior and after APP application showed a substantial increase in surface energy (in both polar and disperse components). However, this more pronounced for the polar component, which presented an over 10-fold increase. The XPS results showed that surface elemental chemistry was modified by the 60s Ar-based APP treatment, and that this change resulted in higher degree of exposure of the surface chemical elements mainly at the expense of the removal of adsorbed C

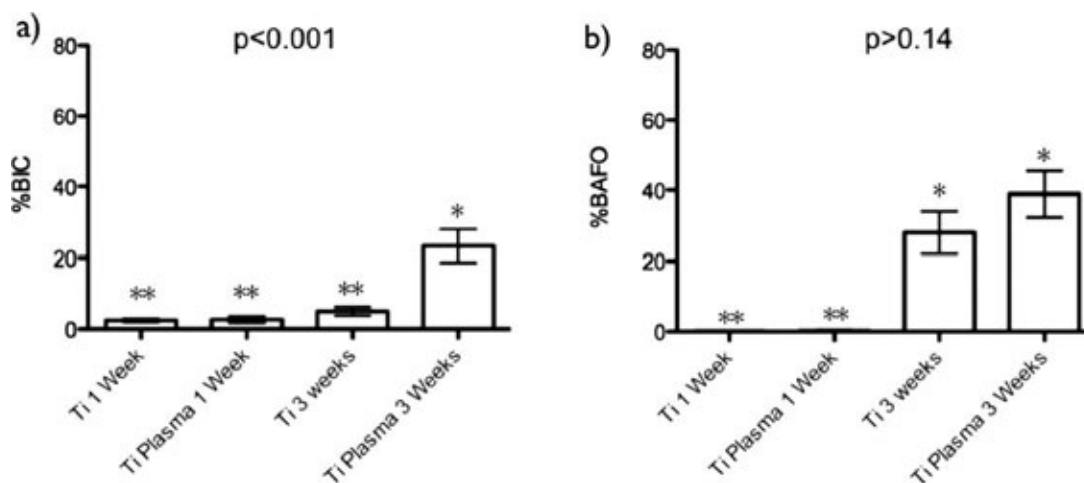


**FIGURE 3.** (a) Bone to implant contact (BIC) and (b) bone area fraction occupancy (BAFO) percentages for the Ti and Ti-Plasma groups in the different experimental periods. Results shown as mean  $\pm$  95% confidence interval. The number of asterisks depict statistically homogeneous groups.

species.<sup>8</sup> The higher degree of surface energy observed for the Ti-Plasma is likely related to the removal of the adsorbed C species from the surface.<sup>18–20</sup>

For the *in vivo* model, implants that presented healing chambers leading to the intramembranous-like ossification pathway were utilized. Such healing chambers arise from the interplay between the surgical drilling diameter that matches the outer diameter of the press fit implant circular fins,<sup>21–26</sup> resulting in void spaces between the implant and the osteotomy which are filled with a blood clot immediately after implant placement.<sup>27,28</sup> Our histomorphologic results are in direct agreement with previous work that demonstrated that after a few days, large blood clots filling large healing chambers<sup>29</sup> or the regions between bone and implant healing chamber walls<sup>27,28</sup> will evolve towards a provisional matrix of connective tissue presenting high content of mesenchymal cells (as observed for both experimental groups at 1 week *in vivo*). This stroma will then serve as a scaffold for an intramembranous-like ossification, which was observed at 3 weeks *in vivo*.

The laboratory *in vivo* model results showed key morphologic differences between Ti and Ti-Plasma groups at 1 week *in vivo* at the region within the healing chambers, and such morphologic difference likely accounted for the significantly higher results observed for the Ti-Plasma group at 3 weeks *in vivo*. The morphologic difference observed at 1 week was likely due to the higher surface wettability observed for the Ti-Plasma group, which resulted in improved blood clot adherence and closer interaction between the connective tissue matrix with the implant surface, which likely arose from the higher degrees of surface energy observed for that surface. Such closer interaction then prevented the connective tissue network from collapsing to the central area of the healing chamber (only observed for the Ti group at 1 week). The more uniform presence of osteogenic tissue throughout the chamber and closer interaction with the implant surface observed for the Ti-Plasma group at 1 week possibly resulted in the significantly higher degrees of BIC (over 300%)

and higher mean BAFO (~30%) at 3 weeks observed for the Ti-Plasma group. These results are in agreement with previous work that showed that surface wettability is beneficial in hastening osseointegration in healing chambers at early times *in vivo*.<sup>30</sup>

## CONCLUSIONS

Since the role of surface energy on osteoblast function is well understood to enhance adhesion, proliferation, mineralization,<sup>31–34</sup> and thus potentially the quantity and quality of initial bone healing, it is highly desirable to increase the wettability of implantable devices.<sup>30</sup> As per our results, doing so by means of APP treatment fostered higher levels of contact with the surrounding tissues during the crucial initial healing stages, promoting more rapid and higher-quantity bone around rough titanium surfaces. The application of APP appears to be a viable large-scale alternative process relative to other proprietary fabrication techniques such as surface cleaning and storage in isotonic solution has been previously shown to hasten osseointegration of dental implants at early implantation times.<sup>30</sup>

## REFERENCES

- Coelho PG, Granjeiro JM, Romanos GE, Suzuki M, Silva NR, Cardaropoli G, Thompson VP, Lemons JE. Basic research methods and current trends of dental implant surfaces. *J Biomed Mater Res Part B Appl Biomater* 2009;88:579–596.
- Jimbo R, Sawase T, Shibata Y, Hirata K, Hishikawa Y, Tanaka Y, Bessho K, Ikeda T, Atsuta M. Enhanced osseointegration by the chemotactic activity of plasma fibronectin for cellular fibronectin positive cells. *Biomaterials* 2007;28:3469–3477.
- Coelho PG, Granjeiro JM, Romanos GE, Suzuki M, Silva NR, Cardaropoli G, Thompson VP, Lemons JE. Basic research methods and current trends of dental implant surfaces. *J Biomed Mater Res B Appl Biomater* 2009;88:579–596.
- Dohan Ehrenfest DM, Coelho PG, Kang BS, Sul YT, Albrektsson T. Classification of osseointegrated implant surfaces: Materials, chemistry and topography. *Trends Biotechnol* 2010;28:198–206.
- Albrektsson T, Wennerberg A. Oral implant surfaces, Part 1—Review focusing on topographic and chemical properties of different surfaces and *in vivo* responses to them. *Int J Prosthodont* 2004;17:536–543.

6. Albrektsson T, Wennerberg A. Oral implant surfaces, Part 2—Review focusing on clinical knowledge of different surfaces. *Int J Prosthodont* 2004;17:544–564.
7. Kang BS, Sul YT, Oh SJ, Lee HJ, Albrektsson T. XPS, AES and SEM analysis of recent dental implants. *Acta Biomater* 2009;5:2222–2229.
8. Coelho PG, Lemons JE. Physico/chemical characterization and in vivo evaluation of nanothickness bioceramic depositions on alumina-blasted/acid-etched Ti-6Al-4V implant surfaces. *J Biomed Mater Res A* 2009;90:351–361.
9. Granato R, Marin C, Gil JN, Chuang SK, Dodson TB, Suzuki M, Coelho PG. Thin bioactive ceramic-coated alumina-blasted/acid-etched implant surface enhances biomechanical fixation of implants: An experimental study in dogs. *Clin Implant Dent Relat Res* 2011;13:87–94. DOI: 10.1111/j.1708-8208.2009.00186.x.
10. Marin C, Granato R, Suzuki M, Gil JN, Piattelli A, Coelho PG. Removal torque and histomorphometric evaluation of bioceramic grit-blasted/acid-etched and dual acid-etched implant surfaces: An experimental study in dogs. *J Periodontol* 2008;79:1942–1949.
11. Lieberman MA, Lichtenberg AJ. *Principles of Plasma Discharges and Materials Processing*. New York: Wiley; 1994.
12. Barker R. Introduction and overview. In: Becker UK, Schoenbach KH, Barker RJ, editors. *Non-Equilibrium Air Plasmas at Atmospheric Pressure*. Bristol: IOP Publishing; 2005.
13. Liu F, Sun P, Bai N, Tian Y, Zhou H, Wei S, Zhou Y, Zhang J, Zhu W, Becker K, Fan J. Inactivation of bacteria in an aqueous environment by a direct-current, cold atmospheric-pressure air plasma microjet. *Plasma Proc Polym* 2010;7:231–236.
14. Foest R, Kindel E, Lange H, Ohl A, Stieber M, Weltmann K-D. *Plasma Phys Contr. Fusion* 2005;47:B525–B536.
15. Foest R, Schmidt M, Becker K. Microplasmas, a New World of low-temperature plasmas. *Int J Mass Spectrom* 2005;248:87–102.
16. Owens DK, Wendt RC. Estimation of the surface free energy of polymers. *J Appl Polym Sci* 1969;13:1741–1747.
17. Leonard G, Coelho P, Polyzois I, Stassen L, Claffey N. A study of the bone healing kinetics of plateau versus screw root design titanium dental implants. *Clin Oral Implants Res* 2009;20:232–239.
18. Baier RE. Implant dentistry forefront '85. Surface preparation. *J Oral Implantol* 1986;12:389–395.
19. Baier RE. Selected methods of investigation for blood-contact surfaces. *Ann NY Acad Sci* 1987;516:68–77.
20. Baier RE, Meyer AE. Implant surface preparation. *Int J Oral Maxillofac Implants* 1988;3:9–20.
21. Giro G, Marin C, Granato R, Bonfante EA, Suzuki M, Janal MN, Coelho PG. Effect of drilling technique on the early integration of plateau root form endosteal implants: An experimental study in dogs. *J Oral Maxillofac Surg* 2011;69:2158–2163.
22. Suzuki M, Calasans-Maia MD, Marin C, Granato R, Gil JN, Granjeiro JM, Coelho PG. Effect of surface modifications on early bone healing around plateau root form implants: An experimental study in rabbits. *J Oral Maxillofac Surg* 2010;68:1631–1638.
23. Coelho PG, Granato R, Marin C, Bonfante EA, Janal MN, Suzuki M. Biomechanical and bone histomorphologic evaluation of four surfaces on plateau root form implants: An experimental study in dogs. *Oral Surg Oral Med Oral Pathol Oral Radiol Endod* 2010;109:e39–e45.
24. Marin C, Granato R, Suzuki M, Gil JN, Janal MN, Coelho PG. Histomorphologic and histomorphometric evaluation of various endosseous implant healing chamber configurations at early implantation times: A study in dogs. *Clin Oral Implants Res* 2010;21:577–583.
25. Granato R, Marin C, Gil JN, Chuang SK, Dodson TB, Suzuki M, Coelho PG. Thin bioactive ceramic-coated alumina-blasted/acid-etched implant surface enhances biomechanical fixation of implants: An experimental study in dogs. *Clin Implant Dent Relat Res* 2011;13:87–94.
26. Coelho PG, Marin C, Granato R, Suzuki M. Histomorphologic analysis of 30 plateau root form implants retrieved after 8 to 13 years in function. A human retrieval study. *J Biomed Mater Res B Appl Biomater* 2009;91:975–979.
27. Berglundh T, Abrahamsson I, Albohy JP, Lindhe J. Bone healing at implants with a fluoride-modified surface: An experimental study in dogs. *Clin Oral Implants Res* 2007;18:147–152.
28. Berglundh T, Abrahamsson I, Lang NP, Lindhe J. De novo alveolar bone formation adjacent to endosseous implants. *Clin Oral Implants Res* 2003;14:251–262.
29. Cardaropoli G, Wennstrom JL, Lekholm U. Peri-implant bone alterations in relation to inter-unit distances. A 3-year retrospective study. *Clin Oral Implants Res* 2003;14:430–436.
30. Buser D, Broggin N, Wieland M, Schenk RK, Denzer AJ, Cochran DL, Hoffmann B, Lussi A, Steinemann SG. Enhanced bone apposition to a chemically modified SLA titanium surface. *J Dent Res* 2004;83:529–533.
31. Lai HC, Zhuang LF, Liu X, Wieland M, Zhang ZY. The influence of surface energy on early adherent events of osteoblast on titanium substrates. *J Biomed Mater Res Part A* 2010;93:289–296.
32. Lim JY, Liu X, Vogler EA, Donahue HJ. Systematic variation in osteoblast adhesion and phenotype with substratum surface characteristics. *J Biomed Mater Res Part A* 2004;68:504–512.
33. Lim JY, Shaughnessy MC, Zhou Z, Noh H, Vogler EA, Donahue HJ. Surface energy effects on osteoblast spatial growth and mineralization. *Biomaterials* 2008;29:1776–1784.
34. Sista S, Wen C, Hodgson PD, Pande G. The influence of surface energy of titanium-zirconium alloy on osteoblast cell functions in vitro. *J Biomed Mater Res Part A* 2011;97A:27–36.